Early Mechanisms of Renal Injury in Hypercholesterolemic or Hypertriglyceridemic Rats

JAAP A. JOLES,* UTA KUNTER,† ULF JANSSEN,† WILHELM KRIZ,‡
TON J. RABELINK,* HEIN A. KOOMANS,* and JÜRGEN FLOEGE†
**Department of Nephrology and Hypertension, University Medical Center, Utrecht, The Netherlands; †Department of Internal Medicine, Medical School, Aachen, Germany; and ‡Laboratory of Anatomy and Cell Biology, Heidelberg University, Germany.*

Abstract. Hyperlipidemia in conjunction with uninephrectomy leads to renal injury in rats. It is unknown whether this is due to mesangial cell or podocyte injury and whether the injuries induced by hypercholesterolemia and hypertriglyceridemia share a similar pathogenesis. Therefore, renal effects of hypercholesterolemia were studied in male rats with dietary hypercholesterolemia compared with rats on a regular diet. Renal effects of hypertriglyceridemia were studied in female Nagase analbuminemic rats (NAR). Hypertriglyceridemia was reduced in NAR by ovariectomy. Both models were studied after uninephrectomy or sham operation. Dietary hypercholesterolemia had little effect on plasma triglycerides, whereas ovariectomy in the NAR had no effect on plasma cholesterol. However, an increase in intermediate density lipoprotein cholesterol was common to both models. Dietary hypercholesterolemia and uninephrectomy separately induced a similar increase in proteinuria after 13 wk, which was additive when these interventions were combined. At this stage, only a minimal increase was present in glomerular α-smooth muscle actin staining, a marker of mesangial cell activation, or in mesangial matrix expansion. Moreover, platelet-derived growth factor-B chain, a marker of mesangial cell proliferation, was not increased. However, podocyte injury was prominent as evidenced by podocytic *de novo* expression of desmin and ultrastructural changes. Glomerular macrophage counts were increased by hypercholesterolemia but not by uninephrectomy, and were not related to the level of proteinuria. Hypertriglyceridemia and uninephrectomy in female NAR induced an increase in proteinuria after 24 wk, which was also associated with an increase in podocyte desmin expression without any mesangial activation and proliferation or matrix accumulation. Hypertriglyceridemia, proteinuria, and the increase in desmin staining were largely prevented by ovariectomy. Interstitial myofibroblast activation and tubulointerstitial injury accompanied proteinuria in both models. These findings indicate that both hypercholesterolemia and hypertriglyceridemia aggravate renal injury primarily via podocyte rather than via mesangial cell damage. Such podocyte injury is accompanied by tubulointerstitial cell activation and injury.

Hypercholesterolemia and hypertriglyceridemia, recognized as contributing to atherosclerosis, are also emerging as risk factors for progression of renal disease (1,2). Hyperlipidemia is believed to contribute to the onset of renal injury by glomerular accumulation of lipids, in particular in the mesangium (3). Both mesangial and glomerular epithelial cells in culture have been reported to take up cholesterol-rich as well as triglyceride-rich lipoproteins (4–7). In a number of models of experimental renal disease, as well as in renal biopsies obtained from patients with a variety of renal diseases, lipid and apolipoprotein deposition, particularly in mesangial cells and macrophages, has been documented (8–10). However, these findings were obtained at stages with extensive renal injury and may have represented secondary effects.

Little information is available documenting early effects of hyperlipidemia on glomerular morphology. One study, in which 4% cholesterol plus 1% cholic acid in the diet was combined with uninephrectomy, documented some tubulointerstitial changes after only 4 wk (increased tubular osteopontin and interstitial transforming growth factor-β [TGF-β] and tissue inhibitor of metalloproteinase-1 staining), but besides proteinuria and glomerular lipid deposition and TGF-β staining, no other early glomerular changes were reported (11). Another study, in which the diet contained 4% cholesterol plus 2% cholic acid, documented glomerular macrophage influx after only 3 d, and glomerular hypertrophy, foam cell formation, and glomerular mesangial matrix expansion after 4 wk (12). In obese Zucker rats, a model with predominant hypertriglyceridemia (13), an increase in glomerular macrophages at 1 mo of age precedes other morphologic changes and albuminuria by up to 2 mo (14). The above reports stress the pathogenetic roles

Received March 29, 1999. Accepted September 3, 1999.
This work was presented in part at the 30th annual meeting of the American Society of Nephrology, November 2–5, 1997, San Antonio, TX, and at the 31st annual meeting of the American Society of Nephrology, October 25–28, 1998, Philadelphia, PA, and has been published in abstract form (*J Am Soc Nephrol* 8: 619A, 1997 and *J Am Soc Nephrol* 9: 498A, 1998).
Correspondence to Dr. Jaap A. Joles, Department of Nephrology and Hypertension (F03.226), University Medical Certer, Utrecht, P.O. Box 85500, 3508 GA Utrecht, The Netherlands. Phone: +31 30 2507329/2535269; Fax: +31 30 2543492; E-mail: Jaap.A.Joles@med.uu.nl
1046-6673/1104-0669
Journal of the American Society of Nephrology

of macrophage influx and mesangial cell activation/injury (as evidenced by glomerular hypertrophy and matrix accumulation) in lipid-induced glomerular damage. However, despite the presence of proteinuria in most of the studies (11,14), podocyte injury has not been studied. In an attempt to determine the relative contributions of these glomerular factors, we used sensitive immunohistologic markers in hyperlipidemic proteinuric rats at presclerotic stages to determine whether hyperlipidemia primarily leads to mesangial cell activation and proliferation and/or podocyte injury and to determine the role of the glomerular macrophage influx. We also examined the tubulointerstitial changes that accompanied these glomerular events.

In addition to the pathogenetic roles of different cell types in lipid-induced renal damage, it is also unclear whether hypercholesterolemia and hypertriglyceridemia have different effects on renal function and structure, because the renal effects of these forms of hyperlipidemia have never been directly compared. Therefore, two different rodent models were studied. Effects of hypercholesterolemia, particularly of elevated VLDL and IDL cholesterol, were studied in male Sprague Dawley rats with 2% cholesterol and 0.5% cholic acid in their diet (15). Effects of hypertriglyceridemia were studied in female analbuminemic rats compared with ovariectomized counterparts. The Nagase analbuminemic rat (NAR) is a mutant Sprague Dawley rat (16). Female analbuminemic rats are hyperlipidemic (9,16), and ovariectomy decreases plasma triglycerides without affecting cholesterol, which is mainly HDL cholesterol (8). Ovariectomy prevented renal disease in aging (8) and uninephrectomized (17) female analbuminemic rats. Finally, because the development of renal injury is generally accelerated by uninephrectomy (9,18), studies in both models were performed in sham-operated (two-kidney) and uninephrectomized rats.

Materials and Methods

Animals

Male Sprague Dawley rats ($n = 32$) weighing about 250 g were purchased from Harlan-Olac (Blackthorn, United Kingdom). All of these rats underwent surgery under Hypnorm®-Diazepam® anesthesia and sterile conditions. Eight rats were sham-operated and fed a standard diet (2k-con). This natural diet (RMH-TM; Hope Farms, Woerden, The Netherlands) contains 20% digestible protein. Eight rats were sham-operated and fed a standard diet to which 2% cholesterol and 0.5% taurocholate had been added (2k-hychol), eight underwent right nephrectomy and were fed a standard diet (1k-con), and eight underwent right nephrectomy and were fed a standard diet with 2% cholesterol and 0.5% taurocholate (1k-hychol). These rats were studied for 13 wk.

Female NAR ($n = 32$) weighing 200 to 250 g were obtained from our own pathogen-free colony (which was founded with animals generously donated by Dr. S. Nagase, Tokyo, Japan). All of these rats also underwent surgery under the aforementioned conditions. Eight rats were sham-operated (2k-female), eight were bilaterally ovariectomized (2k-ovx), eight underwent right nephrectomy (1k-female), and eight underwent both bilateral ovariectomy and right nephrectomy (1k-ovx). The rats were studied for 24 wk and all were fed a standard diet.

The rats were housed behind barriers. Sentinel animals that were monitored regularly for infection by nematodes and pathogenic bacteria, as well as antibodies to a large number of rodent viral pathogens (International Council of Laboratory Animal Science, Nijmegen, The Netherlands), were consistently negative throughout the experiment. Water and food were available *ad libitum*. The protocol was approved by the Utrecht University Board for study in experimental animals.

Renal Function, BP, and Biochemical Analyses

Urine was collected for determination of urinary protein and creatinine excretion at regular intervals, with the last collection taken 1 wk before sacrifice. The rats were weighed and placed in macrolon metabolism cages with free access to food and water. Tail-cuff pressure was measured in conscious animals in the last week of the protocol (IITC, San Diego, CA). Plasma and urinary protein were determined by the Bradford method using an albumin/globulin standard (Sigma, St. Louis, MO). Urinary albumin was determined by electroimmunoassay, using a rat albumin standard (Sigma). Plasma and urinary creatinine were determined colorimetrically (Sigma). Plasma cholesterol and triglycerides were determined enzymatically (Boehringer-Mannheim, Mannheim, Germany).

Lipoprotein Isolation by Density-Gradient Ultracentrifugation

In nonfasting rats, plasma lipoproteins were separated by density-gradient ultracentrifugation into five fractions (chylomicrons and VLDL, $d < 1.006$ g/ml; IDL, $d = 1.006$ to 1.019 g/ml; LDL_1, $d = 1.019$ to 1.04 g/ml and LDL_2, $d = 1.04$ to 1.063 g/ml; HDL, $d = 1.063$ to 1.21 g/ml). The subdivision of LDL into LDL_1 and LDL_2 was performed to separate the apo B-containing lipoproteins from the other particles present in the density range of 1.019 to 1.063 g/ml (19). Lipoprotein cholesterol was measured as described above.

Tissue Processing

One day before the end of the experiment, the rats in the dietary hypercholesterolemia experiment were injected intraperitoneally with BrdU (100 mg/kg; Sigma) to allow assessment of cell proliferation. At the end of the experiments, blood was collected in the fed state by puncture of the abdominal aorta under pentobarbital anesthesia (60 mg/kg). Subsequently, a 2- to 3-mm slice of the left kidney was collected and fixed in methyl Carnoy's solution (20) and embedded in paraffin for immunohistology. In two to three rats in each subgroup, the left kidney was perfused for about 2 min at 200 mmHg with 1.5% glutaraldehyde in phosphate-buffered saline (PBS) for ultrathin slides and electron microscopy. After continued fixation overnight, the kidney was transferred to a PBS solution until further processing. To avoid exposing tissue destined for immunohistology to glutaraldehyde, the caudal pole of the left kidney was excised before perfusion.

Renal Morphology

Glomerulosclerosis. The percentage of glomeruli exhibiting focal segmental glomerulosclerosis (FSGS) or global glomerulosclerosis was evaluated in the paraffin-embedded material by an observer, who was unaware of the origin of the slides, and was evidenced by segmental increases in glomerular matrix, segmental collapse and obliteration of capillary lumina, and accumulation of hyaline. Such changes were frequently associated with synechial attachments to Bowman's capsule.

Tubulointerstitial Injury. Tubulointerstitial injury was defined as inflammatory cell infiltrates, tubular dilation and/or atrophy, or interstitial fibrosis. Injury was graded according to Shih *et al.* (21) on

a scale of 0 to 4: 0, normal; 0.5, small focal areas of damage; 1, involvement of <10% of the cortex; 2, involvement of 10 to 25% of the cortex; 3, involvement of 25 to 75% of the cortex; 4, extensive damage involving >75% of the cortex.

Transmission Electron Microscopy and High Resolution Light Microscopy

For transmission electron microscopy (TEM) and high-resolution light microscopy (HRLM), slices of renal cortex from perfusion-fixed kidneys were post-fixed in 2% glutaraldehyde-PBS solution overnight, cut into small blocks, and post-fixed in 1% OsO_4 for 2 h. After dehydration in a graded series of ethanol, the samples were embedded in Epon. Semithin 1-μm sections were cut with glass knives on a Reichart Ultracut (NuBlock, Germany), stained with azure II-methylene blue, and examined by light microscopy (Polyvar 2; Reichart). Ultrathin sections were cut with a diamond knife on a Reichart Ultracut, stained with 5% uranyl acetate for 15 min, followed by lead citrate for 2 min, and evaluated in a Phillips EM 301.

Because the overall injury scoring was done in paraffin sections (see above), TEM and HRLM were mainly applied to specify the character of the lesions more precisely. Injury scoring by TEM was not performed. However, most typical lesions defined by TEM could also be detected by HRLM in the 1-μm sections, allowing some quantification of the major lesions (pseudocyst formation, dilation of capillaries, etc.).

Immunoperoxidase Staining

Sections (4 μm) of methyl Carnoy's fixed biopsy tissue were processed by a direct or indirect immunoperoxidase technique as described previously (20,22,23). Primary antibodies included:

- 1A4, a murine monoclonal antibody to a NH_2-terminal synthetic decapeptide of α-smooth muscle actin (Dako, Glostrup, Denmark).
- D33, a murine monoclonal IgG_1 antibody against human muscle desmin (Dako).
- BU-1, a murine monoclonal antibody against 5-bromo-2′-deoxyuridine-containing nuclease in Tris-buffered saline (Amersham, Braunschweig, Germany).
- ED1 (Bioproducts for Science, Indianapolis, IN), a murine monoclonal IgG antibody to a cytoplasmic antigen present in monocytes, macrophages, and dendritic cells.
- Affinity-purified polyclonal goat anti-human/bovine type IV collagen (Southern Biotechnology, Birmingham, AL).
- Affinity-purified IgG fraction of polyclonal rabbit anti-rat fibronectin (Chemicon, Temecula, CA).
- PGF-007 (Mochida Pharmaceutical, Tokyo, Japan), a murine monoclonal antibody to a 25-amino acid peptide located near the COOH terminus of the human platelet-derived growth factor B (PDGF-B) chain.

For all kidneys, negative controls consisted of substitution of the primary antibody with equivalent concentrations of an irrelevant murine monoclonal antibody or normal rabbit or goat IgG. Evaluation of all slides was performed by an observer who was unaware of the origin of the slides.

To obtain mean numbers of proliferating cells or infiltrating monocytes/macrophages in glomeruli, more than 30 consecutive cross sections of glomeruli (range, 30 to 100) were evaluated, and mean values per kidney were calculated. To obtain total counts of proliferating cells or infiltrating monocytes/macrophages in the renal cortex or medulla, more than 30 grid fields (range, 30 to 50) measuring 0.36 mm^2 each were analyzed and, again, mean counts per kidney were obtained. For the evaluation of the immunoperoxidase, each glomerular area for α-smooth muscle actin and PDGF-B chain or each tubulointerstitial grid field stain for α-smooth muscle actin, desmin, type IV collagen, and fibronectin was graded semiquantitatively, and the mean score per biopsy was calculated. Each score reflects mainly changes in the extent rather than intensity of staining and depended on the percentage of the glomerular tuft area or grid field showing positive staining: 0, absent staining or <5% of the area stained; 1, 5 to 25%; 2, 25 to 50%; 3, 50 to 75%; 4, >75%. We and others have recently described that this semiquantitative scoring system is not only reproducible among different observers, but that the data also are highly correlated with those obtained by computerized morphometry (22).

To detect small differences in glomeruli, which might be blunted by the above scoring system, the stains for type IV collagen and fibronectin were evaluated using a point counting method. For this, a grid composed of 121 dots was superimposed on glomeruli (range, 30 to 50; magnification 100-fold), and the percentage of dots overlying stained areas was counted. For desmin, the outer cell layer of the glomerular tuft was evaluated separately. Semiquantitative staining scores in these cases depended on the percentage of the glomerular edge showing positive staining: 0, 0 to 5% stained; 1, 5 to 25%; 2, 25 to 50%; 3, 50 to 75%; 4, >75%.

Immunohistochemical Double-Staining

Double immunostaining for the identification of the type of proliferating cells was performed as reported previously (22) by first staining the sections for proliferating cells with the bromo-deoxyuridine antibody (see above), using an immunoperoxidase procedure. Sections were then incubated with the IgG_1 monoclonal antibody ED-1 against monocytes/macrophages using an immuno-alkaline phosphatase procedure. Cells were identified as proliferating monocytes/macrophages if they showed positive nuclear staining for BrdU and if the nucleus was completely surrounded by cytoplasm positive for the ED-1 antigen. Negative controls included omission of either of the primary antibodies, in which case no double-staining was noted.

Statistical Analyses

Plasma triglycerides and proteinuria were log-normalized to achieve a normal distribution. Results are expressed as arithmetic means ± SEM. Serial data were tested by two-way ANOVA and terminal data by one-way ANOVA. Student-Neuman-Keuls test for multiple comparisons was applied if the variance ratio (F) reached statistical significance ($P < 0.05$).

Results

Male Sprague Dawley Rats: Effects of Hypercholesterolemia Alone

Metabolic and Renal Functional Parameters. Dietary hypercholesterolemia (2k-hychol) alone had no effect on body, kidney, or heart weight, systolic BP, plasma creatinine, or creatinine clearance (Table 1). Plasma cholesterol was more than doubled, but there was only a slight, nonsignificant increase in plasma triglycerides. The cholesterol increase was primarily due to increases in VLDL and IDL, and to a lesser extent LDL_1, whereas LDL_2 and HDL tended to decrease (Table 2). Proteinuria was significantly higher in the 2k-hychol group compared with 2k-con at weeks 10 and 13 (Figure 1). About 50% of the protein loss at week 13 was albumin (Figure 1).

Table 1. Baseline characteristics in male Sprague Dawley rats subjected to either dietary hypercholesterolemia (2k-hychol), uninephrectomy (1k-con), or both (1k-hychol) compared with sham-operated rats on a control diet (2k-con)[a]

Characteristic	2k-Con	2k-Hychol	1k-Con	1k-Hychol
n	8	8	8	8
Body weight (g)	425 ± 8	430 ± 8	397 ± 10[b]	432 ± 9[c]
Liver weight (g)	12.4 ± 0.5	19.8 ± 0.9[c]	12.6 ± 0.3	20.0 ± 0.7[c]
Kidney weight (g)	1.36 ± 0.03	1.48 ± 0.03	1.96 ± 0.06[b]	2.42 ± 0.09[b,c]
Heart weight (g)	1.28 ± 0.05	1.21 ± 0.02	1.27 ± 0.02	1.26 ± 0.03
Systolic BP (mmHg)	161 ± 6	149 ± 4	161 ± 4	160 ± 5
Plasma creatinine (μM)	48 ± 2	46 ± 2	60 ± 3[b]	62 ± 2[b]
C_{Cr} (μl/min)	3167 ± 144	3188 ± 126	2257 ± 124[b]	2285 ± 126[b]

[a] Results are given as mean ±SEM. C_{Cr}, creatinine clearance.
[b] $P < 0.05$ 1k *versus* 2k.
[c] $P < 0.05$ hychol *versus* control diet (con).

Table 2. Plasma lipids and lipoprotein cholesterol in male Sprague Dawley rats subjected to either dietary hypercholesterolemia (2k-hychol), uninephrectomy (1k-con), or both (1k-hychol) compared with sham-operated rats on a control diet (2k-con)[a]

Parameter	2k-Con	2k-Hychol	1k-Con	1k-Hychol
n	8	8	8	8
Cholesterol (mM)	2.08 ± 0.07	4.79 ± 0.59[c]	2.88 ± 0.21[b]	6.87 ± 0.55[b,c]
Triglycerides (mM)	0.59 ± 0.07	0.81 ± 0.10	0.65 ± 0.07	1.12 ± 0.14[b,c]
VLDL (mM)	0.06 ± 0.02	1.93 ± 0.29[c]	0.07 ± 0.03	2.47 ± 0.34[c]
IDL (mM)	0.04 ± 0.02	1.07 ± 0.22[c]	0.02 ± 0.01	1.35 ± 0.27[c]
LDL_1 (mM)	0.21 ± 0.02	0.57 ± 0.05[c]	0.41 ± 0.09	0.86 ± 0.14[b,c]
LDL_2 (mM)	0.36 ± 0.03	0.11 ± 0.01[c]	0.54 ± 0.05[b]	0.20 ± 0.04[c]
HDL (mM)	1.27 ± 0.04	0.99 ± 0.06	1.72 ± 0.12[b]	1.65 ± 0.17[b]

[a] Results are given as mean ± SEM.
[b] $P < 0.05$ 1k *versus* 2k.
[c] $P < 0.05$ hychol *versus* control diet (con).

Immunohistologic Changes. The percentage of glomeruli with FSGS in 2k-hychol rats at week 13 was similar to 2k-con. However, there was a small increase in the tubulointerstitial injury index (Figure 2). Monocyte/macrophage counts were significantly increased in glomeruli and in tubulointerstitium in 2k-hychol rats compared with 2k-con (Figure 2). To specifically investigate cellular injury in the rats, we assessed the glomerular *de novo* expression of α-smooth muscle actin, an indicator of mesangial cell activation (24), *de novo* expression of PDGF-B chain, an indicator of mesangial cell proliferation (23), and the glomerular *de novo* desmin staining, which, particularly at the tuft edge, is a marker of podocyte injury (20,23). In the renal interstitium, *de novo* expression of desmin and α-smooth muscle actin are indicators of myofibroblast transformation (24,25). In 2k-hychol rats, there was no obvious mesangial cell activation as evidenced by the lack of glomerular α-smooth muscle actin expression, cell proliferation, or matrix accumulation (Figure 2). Even the numerical increase in glomerular cell proliferation appeared to be mostly due to local proliferation of monocytes rather than mesangial cells as BrdU+/ED-1+ cells per glomerulus increased from 0.01 ± 0.01 in 2k-con to 0.04 ± 0.01 in 2k-hychol rats ($P < 0.05$), and there was no increase in PDGF-B chain staining (0.94 ± 0.02 in 2k-hychol *versus* 0.85 ± 0.02 in 2k-con, NS). Podocyte desmin expression increased slightly but failed to reach statistical significance over 2k-con (Figure 2 and Figure 3, A and B). Evaluated by HRLM, kidneys from 2k-hychol rats exhibited pseudocysts in 10% of glomeruli (range, 8 to 11%), and in 34% (33 to 35%) dilated glomerular capillaries. However, this was not different from 2k-con, where the incidence of podocytic pseudocysts was 20% (2 to 21%), and 32% (10 to 36%) exhibited dilated glomerular capillaries. By TEM, kidneys from 2k-hychol rats, in addition to widespread pseudocyst formation in podocytes (also seen in controls), showed many podocytes filled with dark staining absorption droplets. Macrophages were occasionally encountered within glomerular capillary lumina (Figure 4A). In the tubulointerstitium, no sign of fibroblast activation was noted, as evidenced by the lack of α-smooth muscle actin or desmin expression, matrix accumulation, or increased cell proliferation (Figure 2).

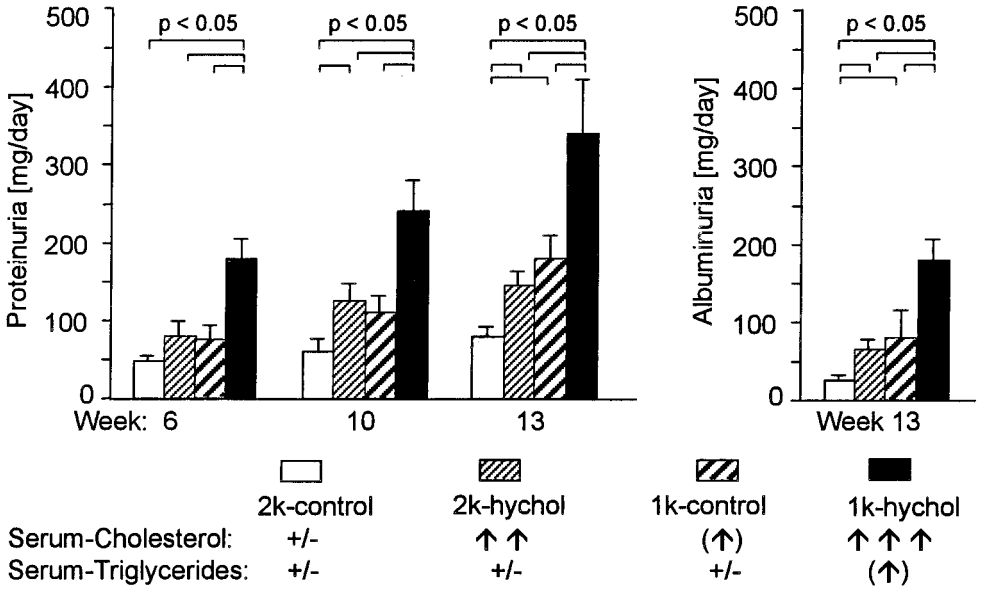

Figure 1. Proteinuria (weeks 6 to 13 post-surgery) and albuminuria (week 13) in male Sprague Dawley rats after sham operation (2k-con), uninephrectomy (1k-con), dietary hypercholesterolemia (2k-hychol), or both (1k-hychol). Results are given as mean ± SEM.

Male Sprague Dawley Rats: Effects of Uninephrectomy Alone

Metabolic and Renal Functional Parameters. Uninephrectomy alone (1k-con) did not affect systolic BP. There was marked renal hypertrophy, and creatinine clearance decreased by 25% (Table 1). Compared with 2k-con rats, plasma cholesterol was mildly increased, but there was no effect on triglycerides. There were no increases in VLDL or IDL, slight increases in LDL_1 and LDL_2, and more marked increases in HDL (Table 2). Proteinuria and albuminuria in 1k-con rats were significantly higher than in 2k-con rats at 13 wk (Figure 1).

Immunohistologic Changes. Comparison of glomerular changes in 1k-con and 2k-con rats showed a significant increase in the percentage of glomeruli with FSGS, some evidence of podocyte activation (*de novo* expression of desmin at the glomerular tuft edge), but no sign of mesangial cell activation (as assessed by α-smooth muscle actin expression and matrix expansion) or monocyte/macrophage influx (Figure 2 and Figure 3C). Using HRLM, we found that 13% of the glomeruli showed podocytic pseudocysts and 36% dilated glomerular capillaries. In the tubulointerstitium, the injury index, desmin expression, and monocyte/macrophage influx were significantly elevated compared with 2k-con rats. There was no increased cell proliferation in either the glomeruli or tubulointerstitium (Figure 2) and no increase in glomerular PDGF-B staining. Thus, uninephrectomy as such did not stimulate persistent glomerular cell proliferation or α-smooth muscle actin staining, and therefore also does not seem to provoke major mesangial cell changes in normotensive, normolipidemic rats.

Male Sprague Dawley Rats: Effects of Hypercholesterolemia plus Uninephrectomy

Metabolic and Renal Functional Parameters. Combining uninephrectomy with hypercholesterolemia (1k-hychol) had no effect on systolic BP. Kidney weight was markedly increased compared with both single intervention groups (Table 1). Adding hypercholesterolemia to uninephrectomy did not cause an additional impairment in creatinine clearance. Both plasma cholesterol and triglycerides were increased compared with all other groups. The increase in cholesterol was due to markedly elevated levels of VLDL, IDL, and LDL_1 (Table 2). LDL_2 decreased, and HDL was not further increased despite the fact that proteinuria and albuminuria were significantly higher than in any other group at every time point (Figure 1).

Immunohistologic Changes. About 20% of the glomeruli showed FSGS, which was significantly higher than the FSGS frequency in both 2k groups (Figure 2). Signs of mesangial cell activation in these rats were minimal. First, glomerular *de novo* expression of α-smooth muscle actin was almost absent and similar to 2k- and 1k-con rats (Figure 5, A and B), albeit significantly elevated in comparison to 2k-hychol rats (Figure 2). Second, glomerular cell proliferation was not significantly different from any other group (Figure 2); moreover, similar to 1k-hychol rats, the numerical increase in glomerular cell proliferation appeared to be due mostly to proliferating monocytes (BrdU+/ED-1+ cell per glomerulus 0.05 ± 0.02 *versus* 0.01 ± 0.01 in 1k-con; $P < 0.05$), and there was no increase in PDGF-B chain (0.94 ± 0.02 in 1k-hychol *versus* 0.88 ± 0.02 in 1k-con, NS). Third, glomerular matrix accumulation, albeit statistically increased over 2k-controls, was minimal (type IV collagen) (Figure 2). In contrast to the lack of mesangial cell activation, signs of podocyte injury were more prominent: Glomerular desmin scores at the edge of the tuft were increased 2.4-fold compared with 2k-controls (Figure 2). Furthermore, with HRLM we found that 39% (25 to 52%) of glomeruli showed podocytic pseudocysts, and 34% (24 to 44%) dilated glomerular capillaries. TEM (Figure 4B) clearly

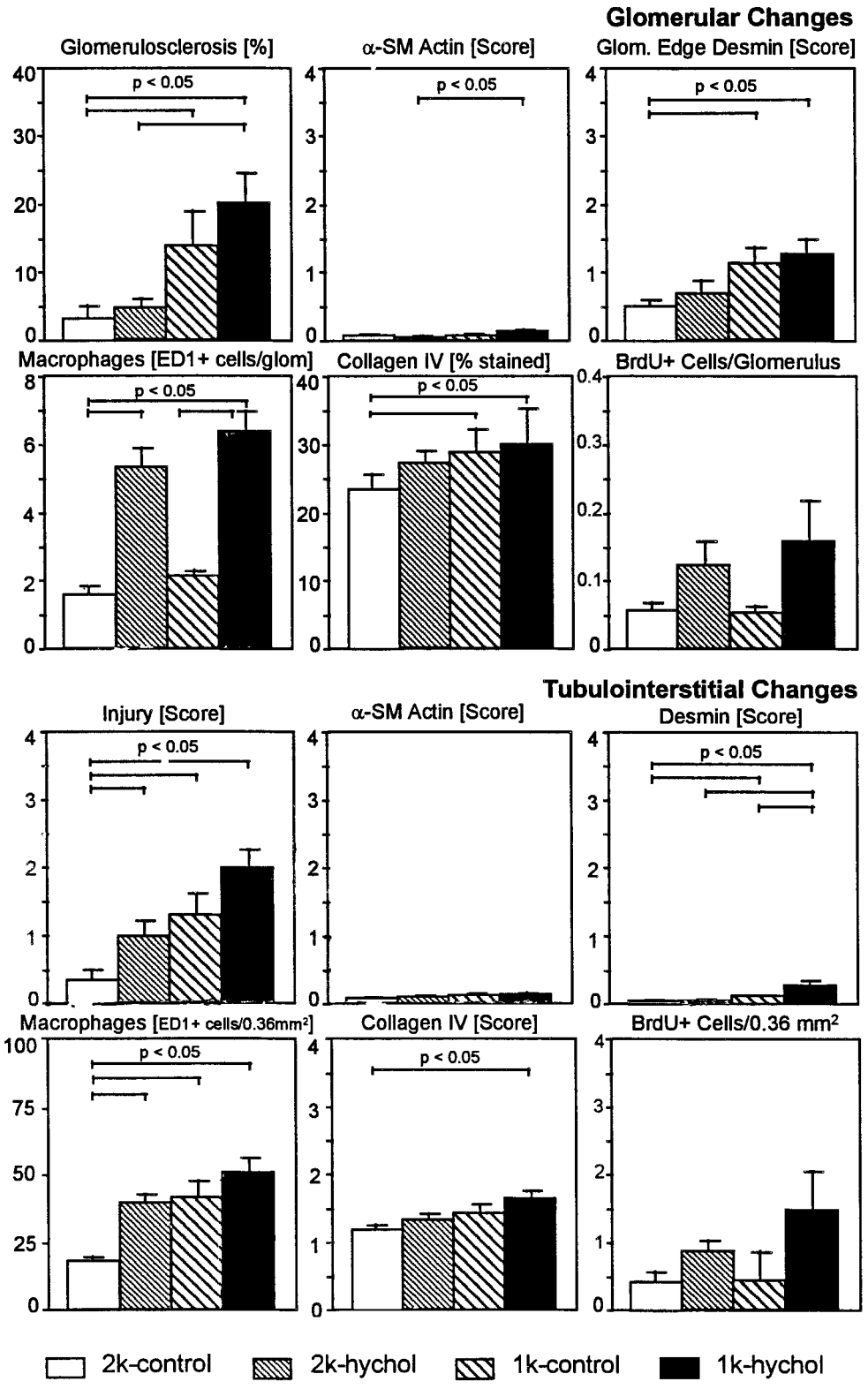

Figure 2. Markers of glomerular and tubulointerstitial injury in male Sprague Dawley rats after sham operation (2k-con), uninephrectomy (1k-con), dietary hypercholesterolemia (2k-hychol), or both (1k-hychol). Results are given as mean ± SEM.

showed the abundant podocyte injuries consisting of foot process effacement, pseudocyst formation, and accumulation of absorption droplets. Occasionally, remnants of podocytes were encountered in Bowman's space, thus indicating detachments from the glomerular basement membrane (GBM). Adjacent to sclerotic tuft portions, naked GBM areas were regularly seen.

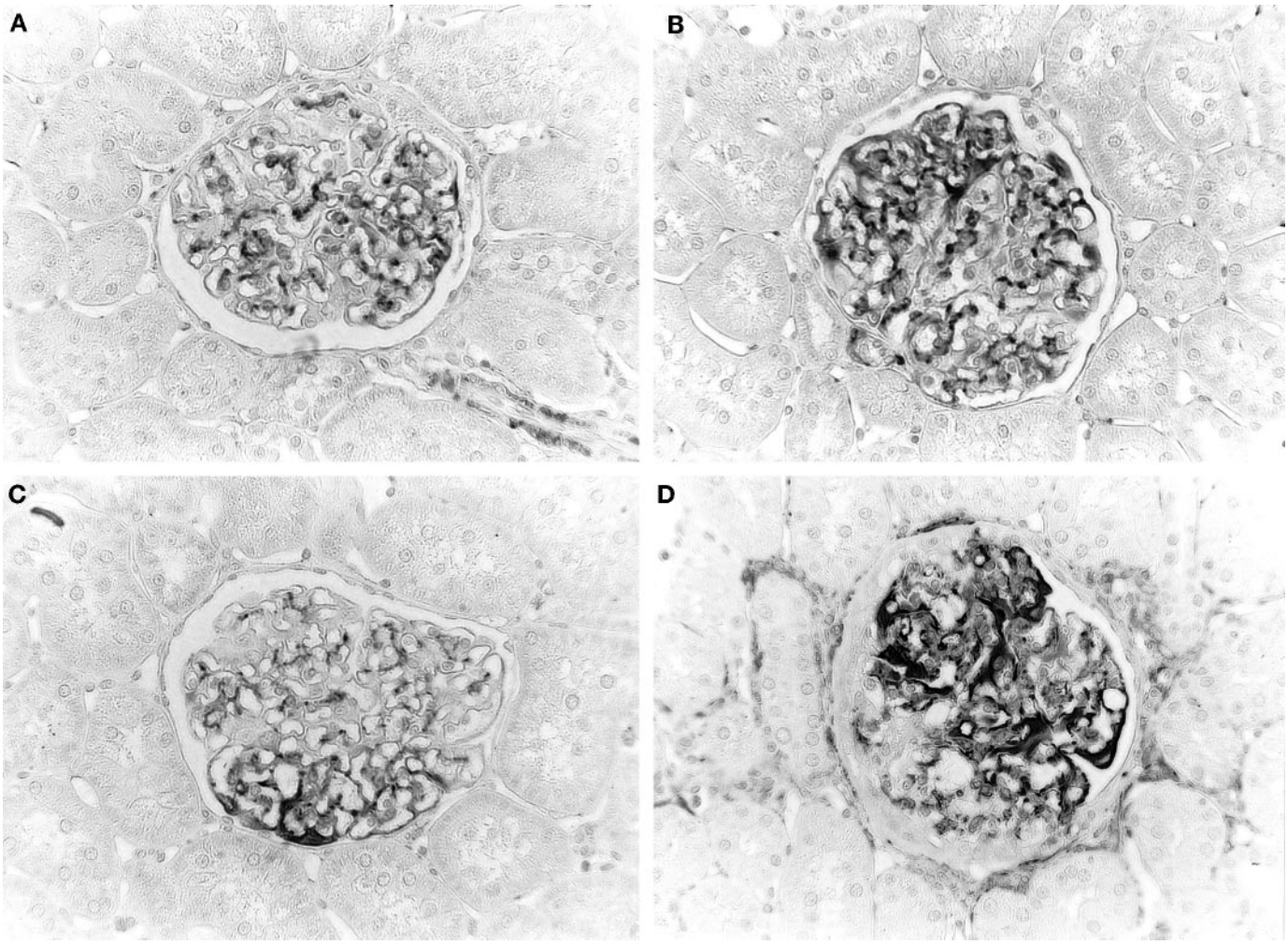

Figure 3. Expression of desmin in male Sprague Dawley rats after sham operation (2k-con), uninephrectomy (1k-con), dietary hypercholesterolemia (2k-hychol), or both (1k-hychol). (A) 2k-con: Baseline glomerular staining and virtual absence of tubulointerstitial staining. (B) 2k-hychol: Marginally increased glomerular staining and virtual absence of tubulointerstitial staining. (C) 1k-con: Increased glomerular staining and slight tubulointerstitial staining. (D) 1k-hychol: Increased glomerular staining and mild tubulointerstitial staining. Magnification, ×400.

Segmental sclerosis consisted of synechia of the tuft with the interstitium. As usual in this type of sclerosis development, the sclerotic tuft portions were enclosed in paraglomerular spaces that were separated from the interstitium proper by layers of sheet-like fibroblast processes. The capillaries inside the adherent tuft portions frequently contained macrophages; others were collapsed or hyalinized. Glomerular monocyte/macrophage counts were elevated to a similar degree as in the 2k-hychol group (Figure 2). The tubulointerstitial injury index was significantly higher than in 2k-controls, but not higher than in either the 2k-hychol or 1k-con group. This was accompanied by significant increases in interstitial desmin expression, macrophage influx, and type IV collagen staining (Figure 2).

Notably, over all of the 32 Sprague Dawley rats, there was a highly significant ($P < 0.001$) correlation between albuminuria and interstitial macrophage counts, whereas such a correlation was absent between albuminuria and glomerular macrophage counts (Figure 6).

Female NAR: Effects of Hypertriglyceridemia Alone

Metabolic and Renal Functional Parameters. Hypertriglyceridemic female NAR (2k-female) (Table 3) represent the hyperlipidemic equivalent of male Sprague Dawley rats subjected to dietary hypercholesterolemia (2k-hychol) (Table 2). Consequently, the ovariectomized female NAR (2k-ovx) (Table 3), which have lower triglyceride levels (17), should be viewed as controls and as the equivalent of the normocholesterolemic male Sprague Dawley rats (2k-con) (Table 2). It should be noted that cholesterol and triglycerides are higher in 2k-ovx NAR than in 2k-con Sprague Dawley, but most of the cholesterol is located in LDL_2 and HDL, particles that do not contain apo B (19). Body weight was much lower in 2k-female than in 2k-ovx NAR, whereas relative kidney weight was significantly increased. There were no effects on systolic BP, plasma creatinine, or creatinine clearance when corrected for body weight (Table 4). There was no effect on total or lipoprotein cholesterol, but as expected triglycerides were increased ($P < 0.05$) (Table 3). Proteinuria was not observed in either 2k-ovx or 2k-female NAR (Figure 7).

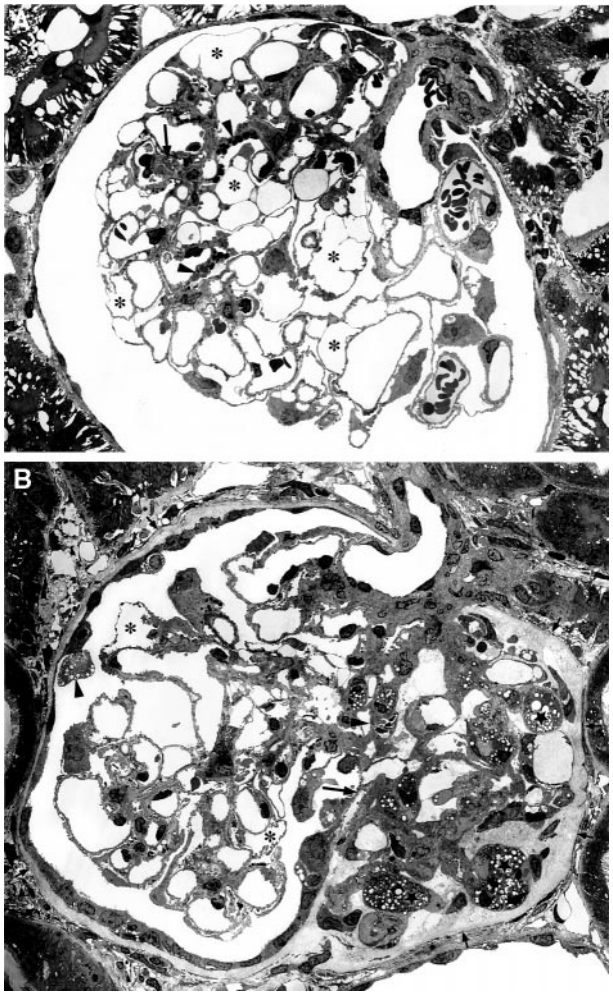

Figure 4. Glomerular lesions as seen by transmission electron microscopy (TEM) in male Sprague Dawley rats after dietary hypercholesterolemia (2k-hychol) or both uninephrectomy and dietary hypercholesterolemia (1k-hychol). (A) Glomerular profile of a 2k-hychol rat. Podocyte damage is seen, including pseudocyst formation (asterisks), foot process effacement, and cytoplasmic accumulation of lysosomal elements (arrowheads). Occasionally, a macrophage within a glomerular capillary is encountered (long arrow). (B) Glomerular profile with segmental sclerosis of a 1k-hychol rat. Within the "intact" lobule of this glomerulus, extensive podocyte injury is seen, ranging from pseudocyst formation (asterisks) to podocyte detachments as recognized either by podocyte remnants or naked glomerular basement membrane (GBM) areas (both labeled by arrowheads). The sclerotic lobule located outside Bowman's capsule is enclosed in a vast paraglomerular space, which already surrounds the entire glomerular profile. The paraglomerular space is separated from the interstitium by a layer of sheet-like fibroblast processes (small arrows). Many of the capillaries within the sclerotic tuft portion contain macrophages (stars). Note separation of the sclerotic from the "intact" tuft portion by parietal epithelium, which flanks the GBM of a collapsed capillary at the flank of the adhesion (long arrow). Magnification: ×710 in A and B.

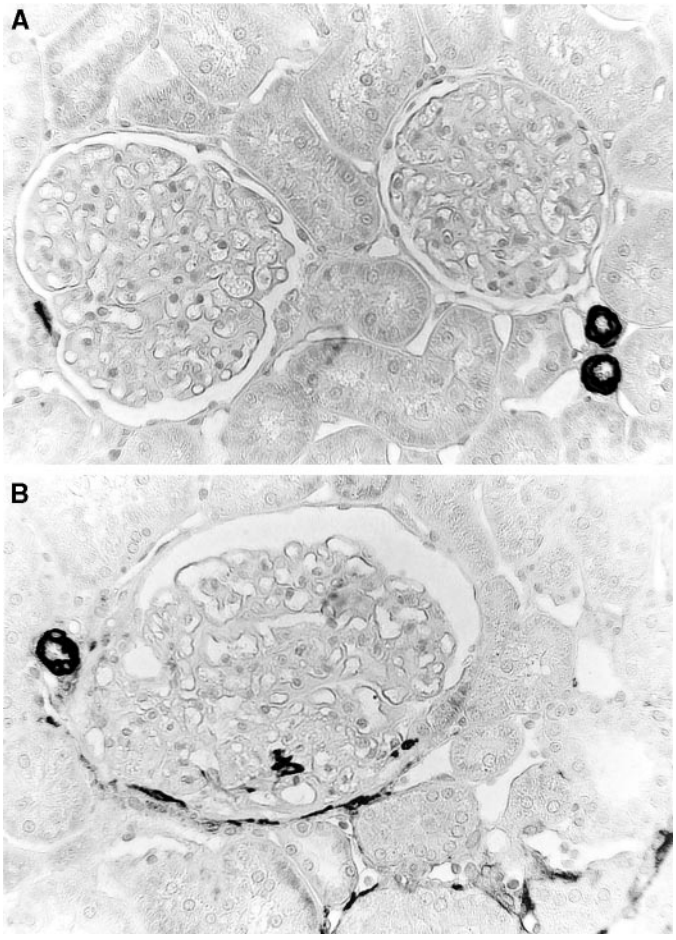

Figure 5. Expression of α-smooth muscle actin in male Sprague Dawley rats after sham operation (2k-con) or uninephrectomy plus dietary hypercholesterolemia (1k-hychol). (A) 2k-con: Absence of both glomerular and tubulointerstitial staining. (B) 1k-hychol: Absence of glomerular and very faint tubulointerstitial staining.

Immunohistologic Changes. Unlike 18-mo-old female NAR, which exhibit widespread glomerular and tubulointerstitial damage (8), the 8-mo-old 2k-female NAR of the present study displayed no signs of glomerular or tubulointerstitial injury (Figure 8).

Ovariectomized Female NAR: Effect of Uninephrectomy Alone

Metabolic and Renal Functional Changes. Uninephrectomized and ovariectomized NAR (1k-ovx) (Table 3), with triglyceride levels very similar to the 2k-ovx, should be viewed as equivalent to the uninephrectomized male Sprague Dawley rats on control chow (1k-con) (Table 2). Uninephrectomy induced renal hypertrophy and hyperfiltration, so that creatinine clearance was about 80% of the value found in the 2k-ovx rats. There was no effect on systolic BP (Table 4). As expected (17), uninephrectomy in ovx NAR did not induce proteinuria (Figure 7). Lipid levels (Table 3) were not affected by uninephrectomy and were very similar to those found in the 2k-ovx group.

Immunohistologic Changes. Glomerular and tubulointerstitial parameters in 1k-ovx NAR were mostly indistinguishable from those in 2k-ovx NAR (Figure 8).

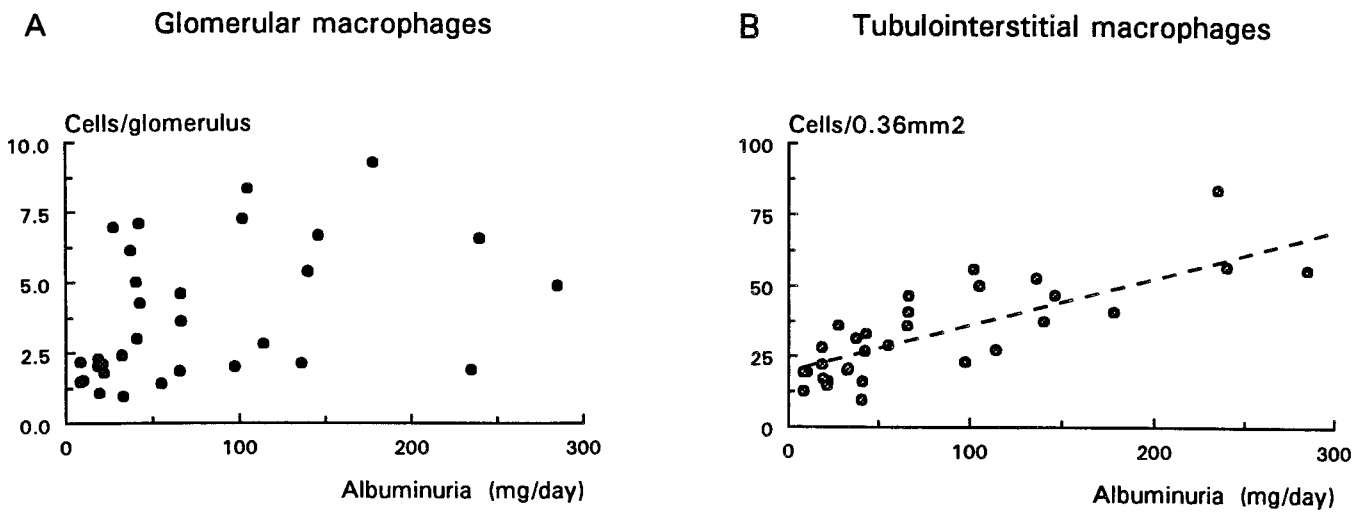

Figure 6. (A) There was no relation between albuminuria and glomerular macrophages ($n = 32$, $P > 0.05$). (B) There was a significant relation between albuminuria and interstitial macrophages ($n = 32$, $P < 0.001$).

Table 3. Plasma lipids and lipoprotein cholesterol in female Nagase analbuminemic rats subjected to either sham operation (2k-female), uninephrectomy plus ovariectomy (1k-ovx), or uninephrectomy (1k-female), compared with ovariectomized (2k-ovx) rats[a]

Parameter	2k-Ovx	2k-Female	1k-Ovx	1k-Female
n	8	8	8	8
Cholesterol (mM)	5.19 ± 0.06	5.12 ± 0.31	5.54 ± 0.30	5.65 ± 0.57
Triglycerides (mM)	2.28 ± 0.18	3.14 ± 0.29[c]	2.12 ± 0.30	4.54 ± 0.38[b,c]
VLDL (mM)	0.28 ± 0.04	0.17 ± 0.03	0.12 ± 0.03	0.23 ± 0.04[c]
IDL (mM)	0.08 ± 0.03	0.18 ± 0.05	0.10 ± 0.05	0.34 ± 0.08[b,c]
LDL_1 (mM)	1.24 ± 0.08	0.85 ± 0.21	1.34 ± 0.14	1.15 ± 0.10
LDL_2 (mM)	0.94 ± 0.05	0.90 ± 0.15	0.93 ± 0.11	0.97 ± 0.08
HDL (mM)	2.65 ± 0.23	2.80 ± 0.13	2.68 ± 0.43	3.21 ± 0.47

[a] Results are given as mean ± SEM.
[b] $P < 0.05$ 1k *versus* 2k.
[c] $P < 0.05$ females *versus* ovx.

Female NAR: Effect of Hypertriglyceridemia and Uninephrectomy

Metabolic and Renal Functional Parameters. Hypertriglyceridemia and uninephrectomy in female NAR (1k-female) (Table 3) should be viewed as the equivalent of hypercholesterolemia and uninephrectomy in male Sprague Dawley rats (1k-hychol) (Table 2). Uninephrectomy (1k-female) in the markedly hypertriglyeridemic female NAR was accompanied by renal hypertrophy and marked hyperfiltration (as indicated by the similar creatinine clearance in 1k and 2k NAR) (Table 4). Systolic BP was also increased by about 20 mmHg ($P < 0.05$). As expected, triglycerides were higher than in 1k-ovx rats. This was accompanied by increases in VLDL and IDL cholesterol (Table 3). Furthermore, triglycerides and IDL cholesterol were also higher than in 2k-females, which was presumably due to the proteinuria, which showed a 10-fold increase at week 24 (Figure 7). However, in absolute terms proteinuria was nearly an order of magnitude lower in the 1k-female NAR than in the 1k-hychol male Sprague Dawley rats, and there were no secondary effects on LDL or HDL.

Immunohistologic Changes. Despite the above difference in proteinuria, the percentage of glomeruli with FSGS was similar: 24 ± 4 in the 1k-female NAR and 20 ± 4 in the 1k-hychol male Sprague Dawley rats. Strong desmin staining was notable in the glomeruli (Figure 8) and accompanied podocytic pseudocysts and dilated glomerular capillaries. As in the 1k-hychol Sprague Dawley males, glomerular α-smooth muscle actin staining (Figure 8) was almost absent in these profoundly hyperlipidemic rats, and there was no change in PDGF-B chain (0.86 ± 0.02 in 1k-female *versus* 0.86 ± 0.02 in 1k-ovx). Glomerular monocyte/macrophage influx was slightly increased in 1k-females compared with 2k-females (Figure 8). Slight but significant increases in glomerular extracellular matrix scores were noted (Figure 8) despite the presence of FSGS in 24% of the glomeruli. This apparent discrepancy was due to the fact that most FSGS lesions were

Table 4. Baseline characteristics in female Nagase analbuminemic rats subjected to either sham operation (2k-female), uninephrectomy plus ovariectomy (1k-ovx), or uninephrectomy (1k-female), compared with ovariectomized (2k-ovx) rats[a]

Characteristic	2k-Ovx	2k-Female	1k-Ovx	1k-Female
n	8	8	8	8
Body weight (g)	326 ± 7	255 ± 11[c]	348 ± 5	263 ± 9[c]
Left kidney weight (g)	0.81 ± 0.02	1.00 ± 0.04	1.40 ± 0.07[b]	1.52 ± 0.09[b]
Left kidney weight (% BW)	0.25 ± 0.00	0.40 ± 0.01[c]	0.41 ± 0.02[b]	0.58 ± 0.03[b,c]
Systolic BP (mmHg)	142 ± 4	139 ± 3	141 ± 4	159 ± 5[b,c]
Plasma creatinine (μM)	55 ± 1	59 ± 4	60 ± 3	53 ± 3
C_{Cr} (μl/min)	2087 ± 115	1648 ± 111[c]	1688 ± 99[b]	1613 ± 81
C_{Cr} (μl/min per 100 g BW)	639 ± 31	639 ± 41	487 ± 30[b]	620 ± 42[c]

[a] Results are given as mean ± SEM. BW, body weight; C_{Cr}, creatinine clearance.
[b] $P < 0.05$ 1k *versus* 2k.
[c] $P < 0.05$ females *versus* ovx.

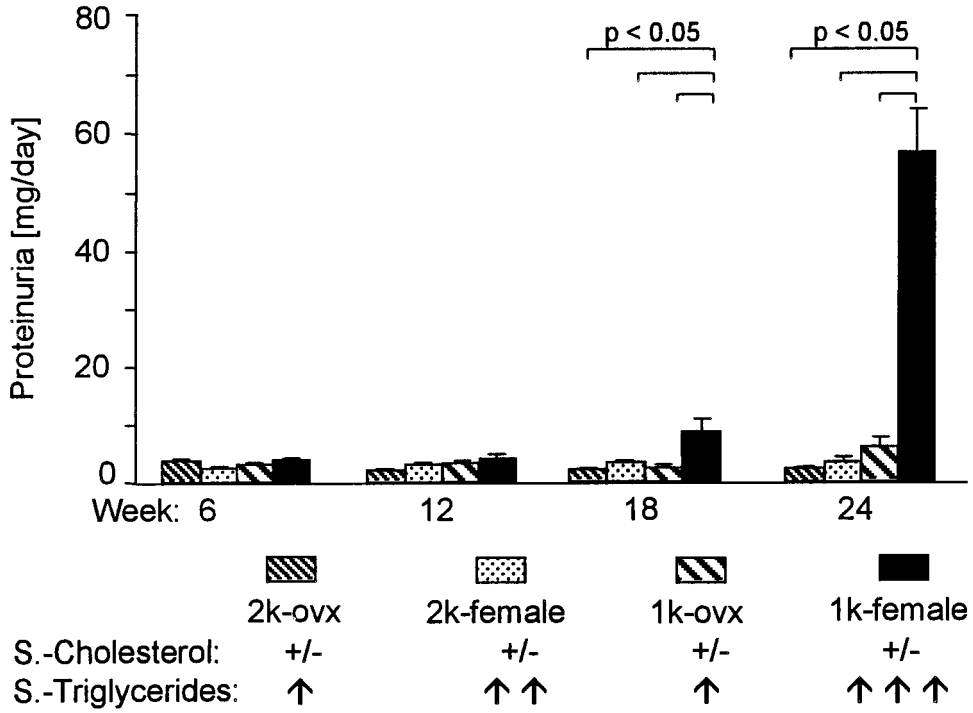

Figure 7. Proteinuria (weeks 6 to 24 post-surgery) in female Nagase analbuminemic rats (NAR) after sham operation (2k-female), uninephrectomy (1k-female), ovariectomy (2k-ovx), or both (1k-ovx). Results are given as mean ± SEM.

still at early stages. By TEM, as in the hypercholesterolemic rats, severe changes were seen after uninephrectomy. Podocyte lesions were widespread and consisted of foot-process effacement, pseudocyst formation, frequent accumulation of absorption droplets, and detachment of podocytes from the GBM (Figure 9). Segmental sclerosis was of the synechia type with sclerotic tuft portions herniating out of Bowman's capsule into a paraglomerular space. Tubulointerstitial lesions were seen in the vicinity of segmentally sclerotic glomeruli. Tubulointerstitial injury in 1k-female rats was present in 10 to 20% of the cortex and was associated with an increase in tubulointerstitial staining of α-smooth muscle actin, matrix components, and some macrophage influx (Figure 8). In contrast to the situation in the male Sprague Dawley rats, female NAR exhibited no correlation between proteinuria and tubulointerstitial monocyte/macrophage counts, possibly because of the much lower level of proteinuria.

Discussion

A central aim of the present study was to investigate early renal events in hypercholesterolemic Sprague Dawley rats and hypertriglyceridemic female NAR that antedate established structural lesions. This aim was achieved in the rats with two kidneys, all of which exhibited little to no glomerulosclerosis

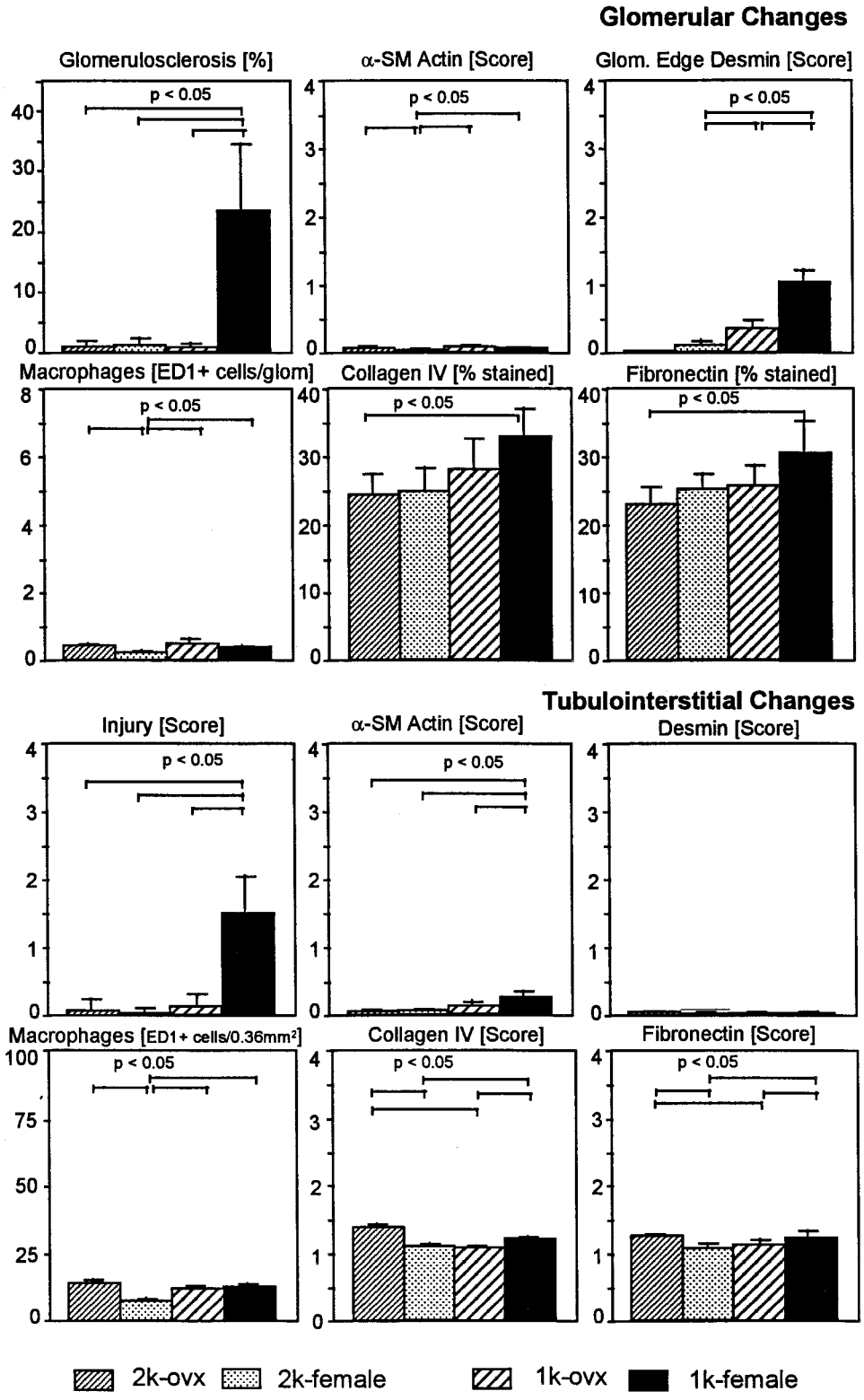

Figure 8. Markers of glomerular and tubulointerstitial injury in female NAR after sham operation (2k-female), uninephrectomy (1k-female), ovariectomy (2k-ovx), or both (1k-ovx). Results are given as mean ± SEM.

or tubulointerstitial injury at the time points investigated. The superposition of renal mass reduction in both situations led to structural renal damage. This combination of experimental situations allowed us to delineate the cellular events that are induced by hyperlipidemia in the kidney.

The first question of the present study was whether hyper-

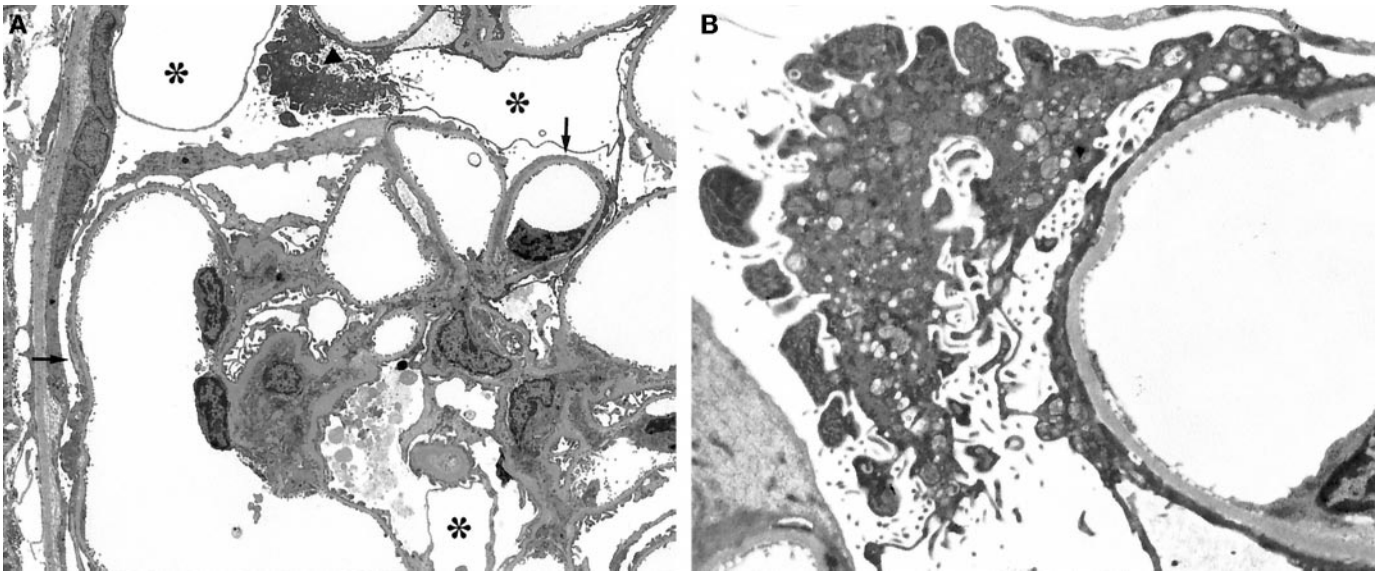

Figure 9. Glomerular lesions as seen by TEM in a female hypertriglyceridemic analbuminemic rat after uninephrectomy (1k-female). (A) Podocyte damage ranges from foot process effacement (arrow) and pseudocyst formation (asterisks) to microvillus transformation of a podocyte with dense cytoplasmic vacuoles filled with laminated structures (arrowhead; shown at higher magnification in B). Magnification: ×1900 in A; ×7200 in B.

cholesterolemia and/or hypertriglyceridemia induce renal damage via an activation of glomerular mesangial cells, as has been suggested on the basis of a large number of cell culture studies. Thus, LDL-receptors are expressed on mesangial cells, both in culture (3) and in biopsies (10). Mesangial cells in culture avidly bind and take up a variety of lipoproteins (3). This has been observed for VLDL (4), IDL (5), LDL (6), and HDL (26). Moreover, after exposure to native as well as oxidized lipoproteins, cultured mesangial cells show increased proliferation (26,27), depressed production of nitric oxide (28) and enhanced production of endothelin (29), growth factors, such as PDGF, TGF-β, and tumor necrosis factor-α (27), as well as structural elements (collagen and fibronectin) (30).

An indicator of mesangial cell activation *in vivo* is the glomerular *de novo* expression of α-smooth muscle actin in both rodents (24) and humans (31), a prominent finding in mesangioproliferative diseases such as immune complex nephritis (32), IgA nephropathy, and diabetic nephropathy (33). Glomerular α-smooth muscle actin staining is also increased in hypertensive nephrosclerosis without mesangial proliferation such as in angiotensin II-mediated hypertension (34) and stroke-prone spontaneously hypertensive rats (35). Such staining was practically absent in both the hypercholesterolemic and the hypertriglyceridemic model, even in the rats with the highest proteinuria and those with combined hyperlipidemia and uninephrectomy. Furthermore, hypercholesterolemia did not have a mitogenic effect in glomeruli. Specifically, there was no mesangial cell proliferation, as evidenced by the absence of increased PDGF-B chain staining. Thus, in the absence of immune-mediated mesangial injury or glomerular hypertension, the mesangium does not seem to play a pivotal role in the development of proteinuria and progression to segmental sclerosis. This assumption is consistent with our recent data in a normotensive rat strain with spontaneous glomerulosclerosis (20).

Direct *in vivo* evidence for lipid-induced mesangial cell activation from other studies is sparse. Although several studies reported mesangial matrix expansion during dietary hypercholesterolemia (12,18), only one actually documented increases in glomerular collagen IV, fibronectin, and laminin content (12). However, in the study of Guijarro *et al.* (12), a much higher dietary content of cholesterol (4%) and cholic acid (2%) was used than in the present study (cholesterol 2% and cholic acid 0.5%). Thus, although our study suggests that lipid-induced renal damage can occur in the absence of significant mesangial cell activation, we cannot exclude that a high-grade dietary cholesterol plus cholic acid challenge might injure mesangial cells *in vivo*.

Given our failure to demonstrate hyperlipidemia-induced mesangial cell activation *in vivo*, we next asked whether podocyte damage does occur under these circumstances. LDL receptors are expressed on podocytes in biopsies (10). Cultured glomerular epithelial cells bind and take up VLDL (2), IDL, and LDL (36). However, similar to findings in cultured mesangial cells, even in the absence of actual uptake of lipoproteins, hyperlipidemia-induced podocyte injury could be related to oxidative stress (37). Thus, after exposure to oxidized lipoproteins, cultured glomerular epithelial cells show enhanced production of TGF-β (38), as well as fibronectin (30,38).

To assess podocyte damage *in vivo*, we used HRLM and TEM, as well as the immunohistochemical demonstration of *de novo* expression of desmin in podocytes. In the normal rat, desmin expression is largely confined to mesangial cells (23), but occurs in podocytes after toxic, hypertensive, or complement-mediated podocyte injury (23) and in rats that spontaneously develop FSGS (20). The data of the present study suggest

that in situations of isolated hyperlipidemia (*i.e.*, 2k-hychol Sprague Dawley rats and 2k-female NAR), slight podocyte damage developed over the time periods studied. Thus, under both conditions, podocyte desmin expression tended to increase, albeit not significantly. Furthermore, significant proteinuria developed in 2k-hychol Sprague Dawley rats (Figure 1), which can serve as indirect evidence of podocyte damage (39). Indeed, by HRLM and TEM, widespread podocyte injury was documented, including (as already observed previously in hyperlipidemic rats; 40) cytoplasmic accumulation of lysosomal elements (absorption droplets) in many podocytes. When hypercholesterolemia and/or hypertriglyceridemia were combined with uninephrectomy, podocyte damage as assessed by the above parameters became striking. Segmental sclerosis developed via the well-characterized podocyte pathway, starting with the formation of tuft adhesions to Bowman's capsule and progressing to broad synechiae (41). Because uninephrectomy *per se* already induced podocyte injury (as demonstrated by HRLM in 1k-control Sprague Dawley rats and 1k-ovx NAR), this suggests that hyperlipidemia primarily acts to aggravate preexisting damage of podocytes. However, it should be noted that aging 2k-female NAR exhibit marked proteinuria and widespread glomerular and tubulointerstitial damage (8).

In the 1k-female NAR, a mild increase in BP was noted, but this probably did not contribute to the marked increase in glomerular desmin staining in this strain because these rats do not exhibit intraglomerular hypertension (9). This latter point is also supported by our observation that α-smooth muscle actin expression was not increased in glomeruli of 1k-NAR, whereas glomerular α-smooth muscle actin expression is markedly augmented in a setting of intraglomerular hypertension (34). Besides reducing triglycerides, ovariectomy conceivably could have other renoprotective effects in NAR. However, no effects of ovariectomy have been found on glomerular diameters (6) or on whole blood viscosity, hyperfiltration, or hyperperfusion after uninephrectomy (17). The 30% increase in body weight is not expected to have a protective effect.

In rats with dietary hypercholesterolemia, glomerular macrophages and plasma cholesterol showed marked parallel increases. However, in female NAR glomerular macrophage numbers were 5 to 10 times lower and not correlated with hypertriglyceridemia. Furthermore, there was no clear association of glomerular macrophage numbers with proteinuria, podocyte damage, or the development of glomerulosclerosis in either the hypercholesterolemic or the hypertriglyceridemic model. Thus, although glomerular macrophage accumulation is certainly an early effect of dietary hypercholesterolemia in rats (11,12,18) and rabbits (42), and has also been observed in hypertriglyceridemic obese Zucker rats (14,43), a pivotal role for macrophages in the pathogenesis of glomerular damage in hyperlipidemic models is not supported by the present study.

Tubulointerstitial injury and macrophage influx, on the other hand, were associated phenomena in the Sprague Dawley rats with hypercholesterolemia, uninephrectomy, or both. This confirms clinical observations (44) as well as findings in other models of glomerular injury, such as membranous nephropathy and renal ablation (45). A common denominator for this observation may be the extent of proteinuria. Thus, albumin (46), transferrin (47), and HDL (48) reabsorption by proximal tubular cells, and the subsequent basolateral secretion of vasoactive and inflammatory substances (48) have been implicated in macrophage chemotaxis and tubular damage. The protective effect of macrophage depletion in hyperlipidemic models by X-irradiation (49) may therefore be causally related to the depletion of tubulointerstitial rather than glomerular macrophages. On the other hand, as suggested previously (50), the link between segmental glomerulosclerosis and tubulointerstitial damage may consist of misdirected filtration and filtrate spreading across the urinary pole onto the outer aspect of the corresponding tubule and surrounding interstitium. Efforts to distinguish between both mechanisms were not undertaken in the present study.

How is it possible that hypercholesterolemia and hypertriglyceridemia both result in relatively uniform morphologic evidence of renal damage? The explanation is probably not that hyperlipidemia in both models was "mixed." Most cholesterol in dietary hypercholesterolemia is in apo B-containing particles, whereas the reverse is true in NAR (15). The highest triglyceride level in rats subjected to dietary cholesterol was $<$50% of that found in the 2k-ovx NAR, and probably secondary to proteinuria (51). One factor that dietary hypercholesterolemia and hypertriglyceridemia in female NAR did have in common was high IDL-cholesterol. In the female NAR, changes in IDL-cholesterol—unlike total cholesterol, LDL-cholesterol, or HDL-cholesterol—were parallel to changes in triglyceride levels (Table 3). IDL is very large and will not be filtered. Thus, it is plausible that injury due to IDL occurs by exposure of the cells forming the glomerular barrier to protein filtration, namely, the capillary endothelium and the visceral epithelium. As mentioned above, cultured glomerular epithelial cells can bind and take up IDL (36).

In summary, no significant mesangial activation or proliferation, as indicated by respectively the absence of *de novo* expression of α-smooth muscle actin or increased PDGF-B chain, was observed in the two different models of experimental hyperlipidemia that are associated with proteinuria, one involving dietary hypercholesterolemia in uninephrectomized male Sprague Dawley rats and the other hypertriglyceridemia in uninephrectomized female analbuminemic rats. In contrast, podocyte and tubulointerstitial injury were present in both models. Our data therefore suggest that in instances of preexisting podocyte activation such as after renal mass reduction, hyperlipidemia contributes to podocyte injury, and that when severe such podocyte damage results in development of the "classic" type of segmental sclerosis associated with secondary damage to the tubulointerstitium.

Acknowledgments

Lipoprotein assays were performed by Nel Willekes-Koolschijn. Tissue processing and staining were performed by Monika Kregeler and Yvonne Schönborn. We acknowledge their expert contributions to this study.

References

1. Muntner PM, Coresh J, Klag MJ, Smith JC, Eckfeldt J: Lipids and incipient hypercreatinemia: A prospective association [Abstract]. *J Am Soc Nephrol* 9: 617, 1998
2. Samuelsson O, Attman P-O, Knight-Gibson C, Larsson R, Mulec H, Weiss L, Alaupovic P: Complex apolipoprotein B-containing lipoprotein particles are associated with a higher rate of progression of human chronic renal insufficiency. *J Am Soc Nephrol* 9: 1482–1488, 1998
3. Wheeler DC, Chana RS: Interactions between lipoproteins, glomerular cells and matrix. *Miner Electrolyte Metab* 19: 149–164, 1993
4. Anami Y, Kobori S, Sakai M, Kasho M, Nishikawa T, Yano T, Matsuda H, Matsumura T, Takemura T, Shichiri M: Human β-migrating very low density lipoprotein induces foam cell formation in human mesangial cells. *Atherosclerosis* 135: 225–234, 1997
5. Kramer-Guth A, Nauck M, Pavenstädt H, Köninger M, Wieland H, Schollmeyer P, Wanner C: Preferential uptake of intermediate-density lipoproteins from nephrotic patients by human mesangial and liver cells. *J Am Soc Nephrol* 5: 1081–1090, 1994
6. Gröne EF, Abboud HE, Höhne M, Walli AK, Gröne, H-J, Stuker D, Robenek H, Wieland E, Seidel S: Actions of lipoproteins in cultured human mesangial cells: Modulation by mitogenic vasoconstrictors. *Am J Physiol* 263: F686–F696, 1992
7. Gröne H-J, Walli A, Gröne E, Krämer A, Clemens MR, Seidel D: Receptor mediated uptake of apo B and apo E rich lipoproteins by human glomerular epithelial cells. *Kidney Int* 37: 1449–1459, 1990
8. Joles JA, van Goor H, van der Horst MLC, van Tol A, Elema JD, Koomans HA: High lipid levels in VLDL and IDL may cause proteinuria and glomerulosclerosis in aging female analbuminemic rats. *Lab Invest* 73: 912–921, 1995
9. Joles JA, van Goor H, Braam B, Willekes-Koolschijn N, Jansen EHJM, van Tol A, Koomans HA: Proteinuria, lipoproteins and renal apolipoprotein deposits in uninephrectomized female analbuminemic rats. *Kidney Int* 47: 442–453, 1995
10. Takemura T, Yoshioka K, Naobumi A, Murakami K, Matumoto A, Itakura H, Kodama T, Suzuki H, Maki S: Apolipoproteins and lipoprotein receptors in glomeruli in human kidney diseases. *Kidney Int* 43: 918–927, 1993
11. Eddy AA: Interstitial inflammation and fibrosis in rats with diet-induced hypercholesterolemia. *Kidney Int* 50: 1139–1149, 1996
12. Guijarro C, Kasiske BL, Kim Y, O'Donnell MP, Lee HS, Keane WF: Early glomerular changes in rats with dietary-induced hypercholesterolemia. *Am J Kidney Dis* 26: 152–161, 1995
13. Kamanna VS, Kirschenbaum MA: Association between very-low-density lipoprotein and glomerular injury in obese Zucker rats. *Am J Nephrol* 13: 53–58, 1993
14. Lavaud S, Michel O, Sassy-Prigent C, Heudes D, Bazin R, Bariety J, Chevalier J: Early influx of glomerular macrophages precedes glomerulosclerosis in the obese Zucker rat model. *J Am Soc Nephrol* 7: 2604–2615, 1996
15. Joles JA, Willekes-Koolschijn N, Scheek LM, Koomans HA, Rabelink TJ, van Tol A: Lipoprotein phospholipid composition and LCAT activity in nephrotic and analbuminemic rats. *Kidney Int* 46: 97–104, 1994
16. Nagase S, Shimamune K, Shumiya S: Albumin-deficient rat mutant. *Science* 205: 590–591, 1979
17. Joles JA, van Goor H, van der Horst MLC, van Tol A, Weening JJ, Koomans HA: Ovariectomy decreases plasma triglycerides and both prevents and alleviates glomerular disease in uninephrectomized female analbuminemic rats. *J Am Soc Nephrol* 7: 1189–1198, 1996
18. Kasiske BL, O'Donnell MP, Schitz PG, Kim Y, Keane WF: Renal injury of diet-induced hypercholesterolemia in rats. *Kidney Int* 37: 880–891, 1990
19. van Tol A, Jansen EHJM, Koomans HA, Joles JA: Hyperlipoproteinemia in Nagase analbuminemic rats. Effects of pravastatin on plasma (apo)lipoproteins and lecithin: Cholesterol acyltransferase activity. *J Lipid Res* 32: 1719–1728, 1991
20. Floege J, Hackmann B, Kliem V, Kriz W, Alpers CE, Johnson RJ, Kühn KW, Koch KM, Brunkhorst R: Age-related glomerulosclerosis and interstitial fibrosis in Milan normotensive rats: A podocyte disease. *Kidney Int* 51: 230–243, 1997
21. Shih W, Hines WH, Neilson EG: Effects of cyclosporin A on the development of immune-mediated interstitial nephritis. *Kidney Int* 33: 1113–1118, 1988
22. Kliem V, Johnson RJ, Alpers CE, Yoshimura A, Couser WG, Koch KM, Floege J: Mechanisms involved in the pathogenesis of tubulointerstitial fibrosis in 5/6-nephrectomized rats. *Kidney Int* 49: 666–678, 1996
23. Floege J, Burns MW, Alpers CE, Yoshimura A, Pritzl P, Gordon K, Seifert RA, Bowen-Pope DF, Couser WG, Johnson RJ: Glomerular cell proliferation and PDGF expression precede glomerulosclerosis in the remnant kidney model. *Kidney Int* 41: 297–309, 1992
24. Johnson RJ, Floege J, Yoshimura A, Iida H, Couser WG, Alpers CE: The activated mesangial cell: A glomerular "myofibroblast"? *J Am Soc Nephrol* 2[Suppl 2]: S190–S197, 1992
25. Diamond JR, van Goor H, Ding G, Engelmyer E: Myofibroblasts in experimental hydronephrosis. *Am J Pathol* 146: 121–129, 1995
26. Neverov NI, Kaysen GA, Nuccitelli R, Weiss RH: HDL causes mesangial cell mitogenesis through a tyrosine kinase-dependent receptor mechanism. *J Am Soc Nephrol* 8: 1247–1256, 1997
27. Nishida Y, Yorioka N, Oda H, Yamakido M: Effect of lipoproteins on cultured human mesangial cells. *Am J Kidney Dis* 29: 919–930, 1997
28. Wu ZL, Liang MY, Qiu LQ: Oxidized low-density lipoprotein decreases the induced nitric oxide synthesis in rat mesangial cells. *Cell Biochem Funct* 16: 153–158, 1998
29. Tan MS, Lee YJ, Shin SJ, Tsai JH: Oxidized low-density lipoprotein stimulates endothelin-1 release and mRNA expression from rat mesangial cells. *J Lab Clin Med* 129: 224–230, 1997
30. Roh DD, Kamanna VS, Kirschenbaum MA: Oxidative modification of low-density lipoprotein enhances mesangial cell protein synthesis and gene expression of extracellular matrix proteins. *Am J Nephrol* 18: 344–350, 1998
31. MacPherson BR, Leslie KO, Lizaro KV, Schwarz JE: Contractile cells of the kidney in primary glomerular disorders: An immunohistochemical study using an anti-α-smooth muscle actin monoclonal antibody. *Hum Pathol* 24: 710–716, 1993
32. Johnson RJ, Iida H, Alpers CE, Majewsky MW, Schwartz SM, Pritzl P, Gordon K, Gown AM: Expression of smooth muscle cell phenotype by rat mesangial cells in immune complex nephritis: α-Smooth muscle actin is a marker of mesangial cell proliferation. *J Clin Invest* 87: 847–858, 1991
33. Alpers CE, Hudkins KL, Gown AM, Johnson RJ: Enhanced expression of "muscle-specific" actin in glomerulonephritis. *Kidney Int* 41: 1134–1142, 1992
34. Johnson RJ, Alpers CE, Yoshimura A, Lombardi D, Pritzl P,

Floege J, Schwartz SM: Renal injury from angiotensin II-mediated hypertension. *Hypertension* 19: 464–474, 1992
35. Kimura K, Suzuki N, Ohba S, Nagai R, Hiroi J, Mise N, Tojo A, Nagaoka A, Hirata Y, Goto A, Yazaki Y, Omata M: Hypertensive glomerular damage as revealed by the expression of α-smooth muscle actin and non-muscle myosin. *Kidney Int* 49[Suppl 55]: S169–S172, 1996
36. Kramer A, Nauck M, Pavenstädt H, Schedler S, Wieland H, Schollmeyer P, Wanner C: Receptor-mediated uptake of IDL and LDL from nephrotic patients by glomerular epithelial cells. *Kidney Int* 44: 1341–1351, 1993
37. Greiber S, Münzel T, Kästner S, Müller B, Schollmeyer P, Pavenstädt H: NAD(P)H oxidase activity in cultured human podocytes: Effects of adenosine triphosphate. *Kidney Int* 53: 654–663, 1998
38. Ding G, van Goor H, Ricardo SD, Orlowski JM, Diamond JR: Oxidized LDL stimulates the expression of TGF-β and fibronectin by glomerular epithelial cells. *Kidney Int* 51: 147–154, 1997
39. Daniels BS: The role of the glomerular epithelial cell in the maintenance of the glomerular filtration barrier. *Am J Nephrol* 13: 318–323, 1993
40. Gröne H-J, Walli A, Gröne E, Niedmann P, Thiery J, Seidel D, Helmchen U: Induction of glomerulosclerosis by dietary lipids: A functional and morphological study in the rat. *Lab Invest* 60: 433–446, 1989
41. Kriz W, Gretz N, Lemley KV: Progression of glomerular diseases: Is the podocyte the culprit? *Kidney Int* 54: 687–698, 1998
42. Yoshimura N, Arima S, Nakayama M, Sato T, Takahashi K: Renal impairment and intraglomerular mononuclear phagocytes in cholesterol-fed rabbits. *Nephron* 68: 473–480, 1994
43. Coimbra TM, Janssen U, Gröne H-J, Ostendorf T, Kunter U, Schmidt H, Brabant G, Floege J: Early events leading to renal injury in obese Zucker (fatty) rats with type II diabetes. *Kidney Int* 57: 167–182, 2000
44. Vleming LJ, de Fijter JW, Westendorp RG, Daha MR, Bruijn JA, van Es LA: Histo-morphometric correlates of renal failure in IgA nephropathy. *Clin Nephrol* 49: 337–344, 1998
45. Abbate M, Zoja C, Corna D, Capitanio M, Bertani T, Remuzzi G: In progressive nephropathies, overload of tubular cells with filtered proteins translates glomerular permeability dysfunction into cellular signals of interstitial inflammation. *J Am Soc Nephrol* 9: 1213–1224, 1998
46. Eddy AA: Interstitial nephritis induced by heterologous protein-overload proteinuria. *Am J Pathol* 135: 719–733, 1989
47. Nankiwell BJ, Tay Y-C, Harris DCH: Dietary protein alters tubular iron accumulation after partial nephrectomy. *Kidney Int* 45: 1006–1013, 1994
48. Ong ACM, Jowett TP, Moorhead JF, Owen JS: Human high density lipoproteins stimulate endothelin-1 release by cultured human renal proximal tubule cells. *Kidney Int* 46: 1315–1321, 1994
49. Diamond JR, Pesek-Diamond I: Sublethal X-irradiation during acute puromycin nephrosis prevents late renal injury: Role of macrophages. *Am J Physiol* 260: F779–F786, 1991
50. Kriz W, Hosser H, Hähnel B, Gretz N, Provoost AP: From segmental glomerulosclerosis to total nephron degeneration and interstitial fibrosis: A histopathological study in rat models and human glomerulopathies. *Nephrol Dial Transplant* 13: 2781–2798, 1998
51. Davies RW, Staprans I, Hutchison FN, Kaysen GA: Proteinuria, not altered albumin metabolism, affects hyperlipidemia in the nephrotic rat. *J Clin Invest* 86: 600–605, 1990